Int. J. Electrochem. Sci., 12 **(2017)** 90 – 102, doi: 1020964/2017.01.09

International Journal of
ELECTROCHEMICAL
SCIENCE
www.electrochemsci.org

Effects of Nano-Sized PbO on the Transport Critical Current Density and Flux Activation Energy of $YBa_2Cu_3O_{7-\delta}$ Superconductor

Annas Al-Sharabi[1], Sarah Yasmin Tajuddin[2], Au Diya Fatihah Wan Saffiey[2], Syazana Jasman[2], H.A. Alwi[2], M.H. Hj Jumali[2], R. Abd-Shukor[2,]*

[1] Department of Physics, Faculty of Applied Sciences, Thamar University, Thamar, Republic of Yemen
[2] School of Applied Physics, Universiti Kebangsaan Malaysia, 43600 Bangi, Selangor, Malaysia
[*]E-mail: ras@ukm.edu.my

Received: 27 September 2016 / *Accepted:* 11 November 2016 / *Published:* 12 December 2016

The effects of nano-sized PbO (10-30 nm) addition on the critical temperature, transport critical current density (J_c) and flux activation energy of $YBa_2Cu_3O_{7-\delta}$ $(PbO)_x$ (x = 0.00-0.45 wt.%), prepared by the standard solid-state reaction method were studied. Powder X-ray diffraction method, electrical resistance measurements and scanning electron microscopy have been used to study the samples. The transport critical current density, J_c was measured using the four-point probe method. The flux activation energy, U was calculated from the resistivity versus temperature measurements using the Arrhenius-type equation. The highest superconducting onset temperature $T_{c\ onset}$ was observed in the sample with x = 0.35 wt. % (94 K). The x = 0.25 wt. % sample showed the highest J_c. The activation energy (U = 0.90 eV) in zero fields showed a maximal plateau between x = 0.20 and 0.35 wt. %. Enhancement of J_c was explained as the increase in the activation energy as a result of nano-sized PbO addition.

Keywords: Activation energy; current density; microstructure; transition temperature

1. INTRODUCTION

The effects of nano-sized particles such as NiO, Y_2O_3, SnO_2, TiO_2 and FeF_2 [1-5] in high T_c superconducting cuprates have been studied to improve the superconducting properties. These particles can react with the superconductor material during processing, as in the case of NiO in $YBa_2Cu_3O_{7-\delta}$ (YBCO) [1]. These particles may generate defects such as twins and inhomogeneous micro-defects, which can act as pinning centers to increase the transport critical current density, J_c.

For a wider application of superconductors a high critical current density is required. The T_c of YBCO remained almost unchanged while the J_c improved remarkably with 0.01 wt.% of nano Al_2O_3 [6]. Flux pinning is important in order to maximize the current density of a superconductor [7]. Many works have been reported on the effect of magnetic field near the superconducting transition in order to understand the pinning mechanism and flux motion [8-10]. Several models to understand the broadening of the resistivity transition curve under magnetic fields, such as thermally activated flux creep [11], flux flow [12], flux line melting and flux cutting [13] have been suggested [8]. Although the Lorentz force exerted on the flux by the current is smaller than the pinning force, the flux line can be thermally activated over the pinning energy barrier. The electrical resistivity region near T_c ($\rho = 0$) can be described by using the thermally activated flux creep model [8, 14-15].

PbO addition is very effective in enhancing the formation of single-phase high temperature superconductor such as in the Tl-based materials [16]. Several methods of synthesizing nano-sized PbO and its properties have been reported ([17] and references therein). In this work we studied the effect of PbO (10-30 nm) additions on the transport critical current density and flux activation energy of $YBa_2Cu_3O_{7-\delta}$. Results of electrical resistivity (dc) measurements, scanning electron microscopy and powder X-ray diffraction are presented. The effects of nano-PbO particle addition in $YBa_2Cu_3O_{7-\delta}$ on J_c and the activation energy are reported in this paper.

2. EXPERIMENTAL DETAILS

The solid-state reaction method has been used to prepare the $YBa_2Cu_3O_{7-\delta}$ $(PbO)_x$ (x = 0, 0.03, 0.05, 0.10, 0.20, 0.25, 0.30 and 0.45 wt.%) samples. High purity (99.9 %) oxides and carbonates such as Y_2O_3, BaO, CuO and nano-sized of PbO (10-30 nm from Nanoshel) were mixed, ground and calcined in air at 900 ^oC for 48 h with one intermediate grinding. The powders were pressed into pellets and sintered in air at 900 ^oC for 24 h. The diameter of the pellets was 13 mm and the thickness was 2.5 mm. The pellets were ground, repelletized and heated at 900 ^oC for another 24 h in order to improve the phase formation.

The dc electrical resistance was measured using the 4-point probe method. Silver paste was used as electrical contact. The van der Pauw method was used to measure the room temperature resistivity. The samples were cut into a bar shape for J_c measurement. The J_c was measured between 30 K and 77 K in zero fields. The 1 μV/cm criterion was used to measure J_c. A CTI Cryogenics Closed Cycle Refrigerator Model 22 was used for low temperature measurements.

The resultant phases was determined by using the powder X-ray diffraction method by employing a Bruker model D8 Advance diffractometer with CuK_α source with wavelength, λ = 1.5418 Å between 2θ = 2 and 60°. At least 15 diffraction peaks were used to calculate the lattice parameters. The microstructure was examined using a Philips XL 30 scanning electron microscope (SEM).

3. RESULTS AND DISCUSSION

Powder X-ray diffraction patterns of $YBa_2Cu_3O_{7-\delta}$ with and without nano-PbO addition are shown in Figure 1. The patterns indicated a single $YBa_2Cu_3O_{7-\delta}$ phase with orthorhombic structure and Pmmm space group. No peaks corresponding to PbO or Pb-based compound were observed in the X-ray diffraction patterns. The lattice constants are shown in Figure 2. The lattice parameters for $x = 0$ are a = 3.819 Å, b = 3.890 Å, and c = 11.67 Å which is in agreement with the literature for pure $YBa_2Cu_3O_{7-\delta}$ [5].

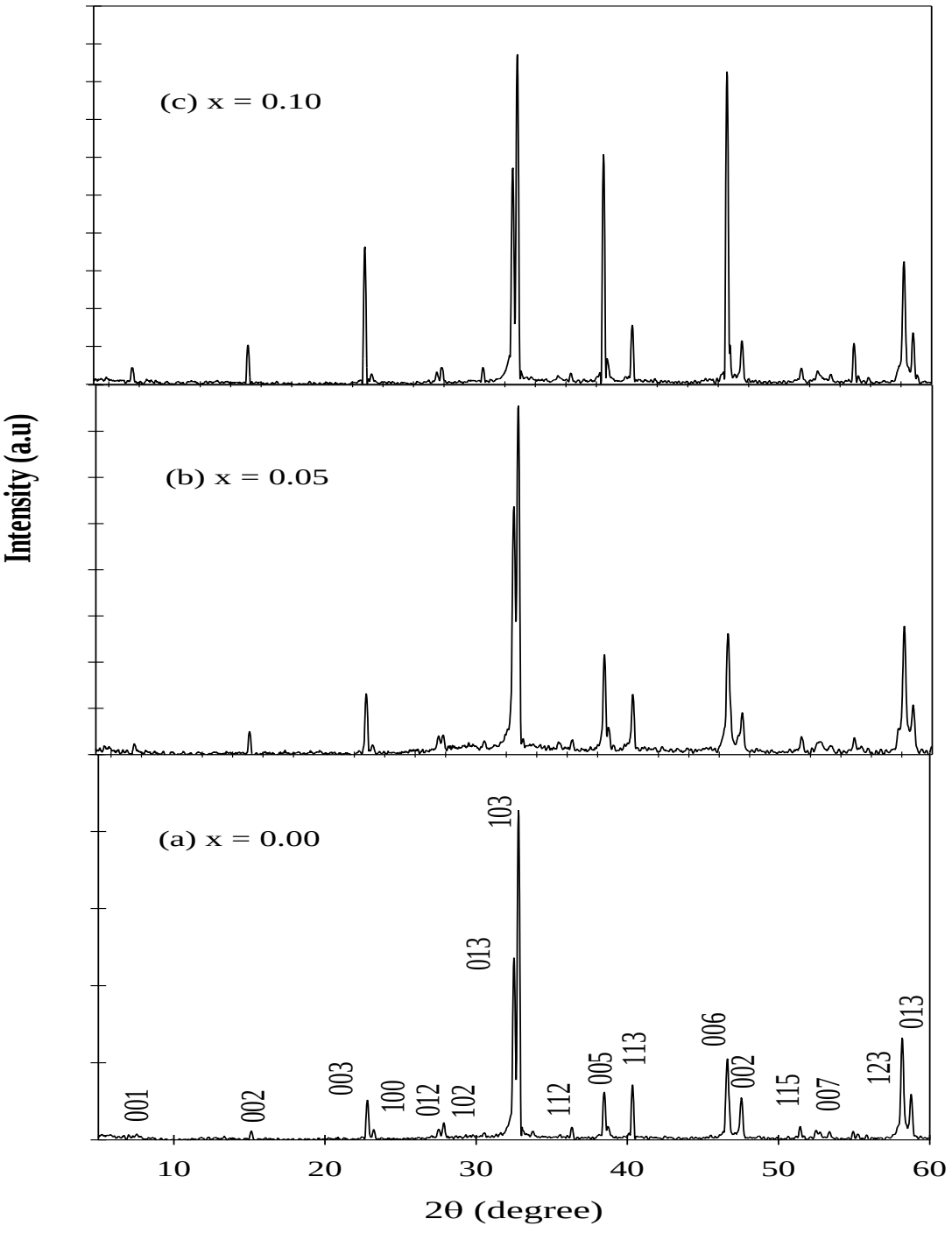

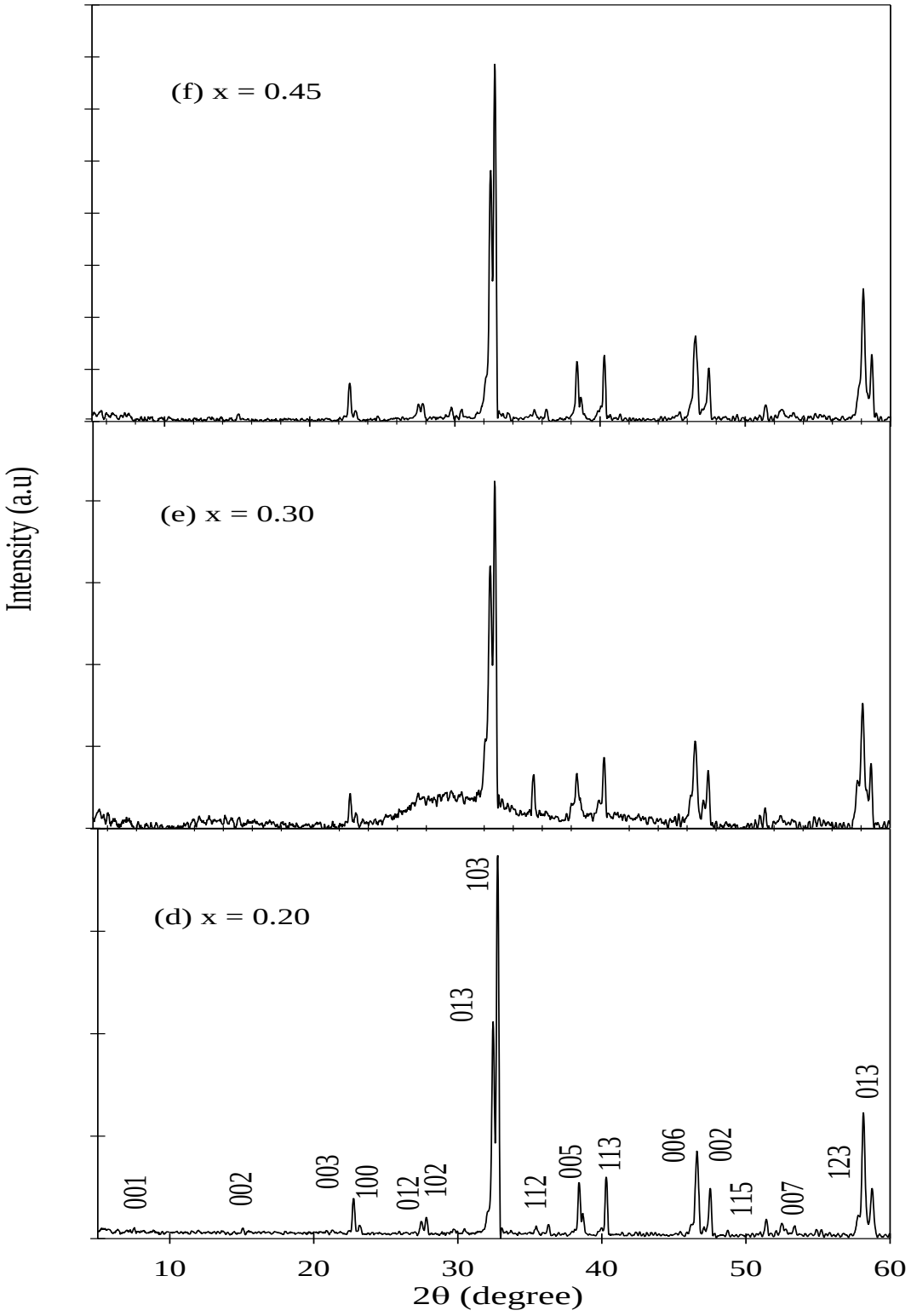

Figure 1. Powder X-ray diffraction patterns for nano-sized PbO added $YBa_2CuO_{7-\delta}$ for x = (a) 0 wt. %, (b) 0.05 wt. %, (c) 0.10 wt. %, (d) 0.20 wt. %, (e) 0.30 wt. % and (f) 0.45 wt. %

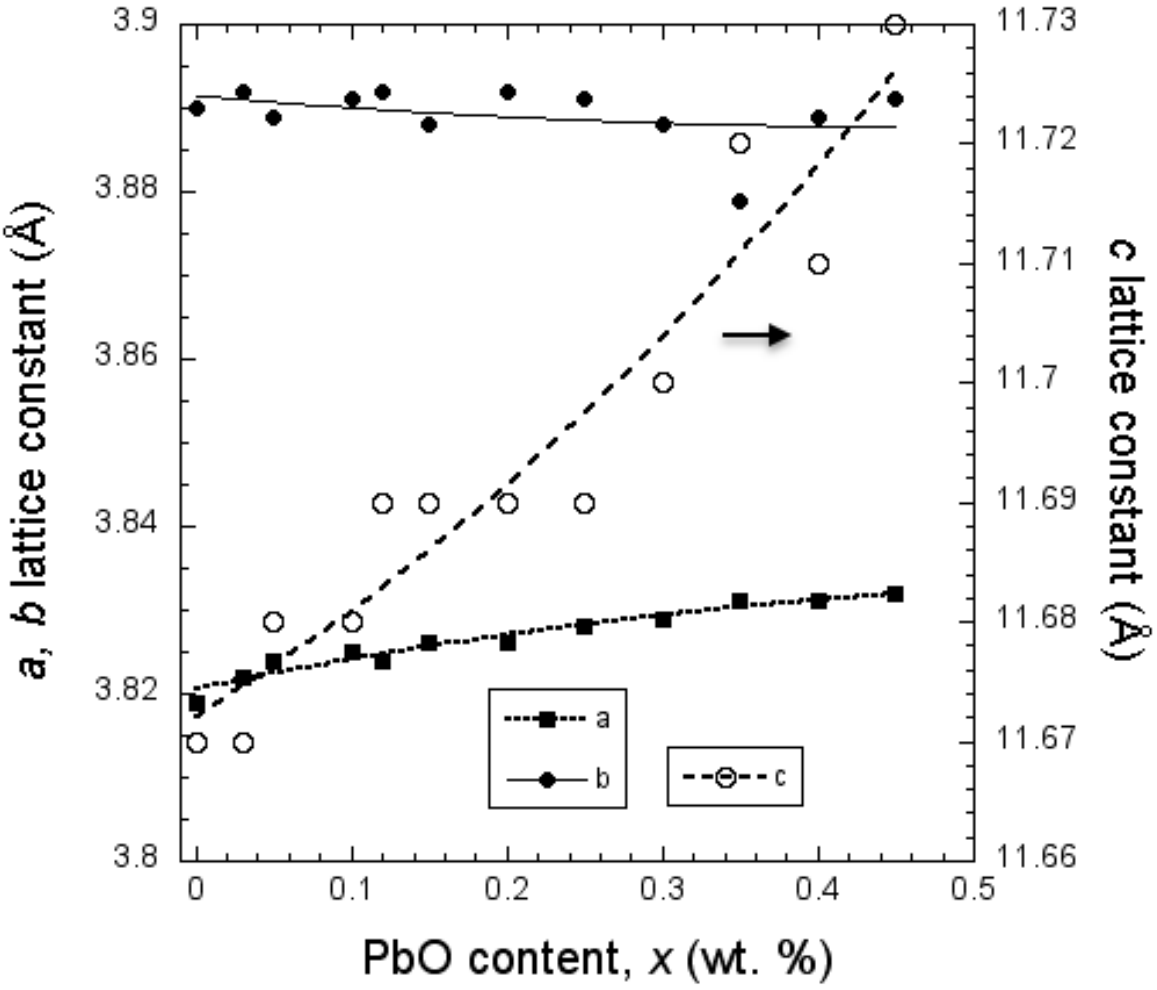

Figure 2. Lattice parameters of nano-sized PbO added $YBa_2CuO_{7-\delta}$

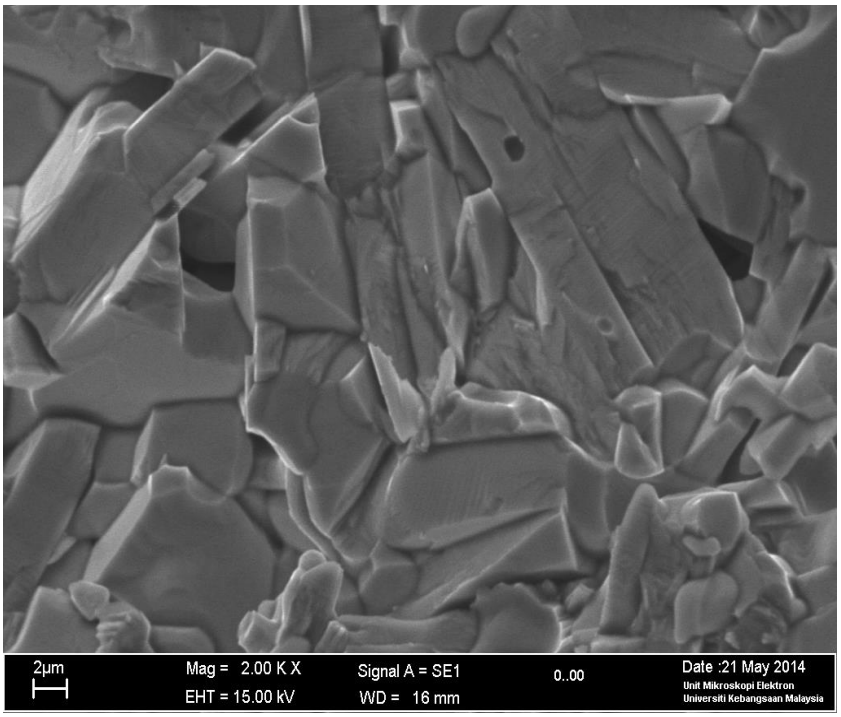

(a) $x = 0$

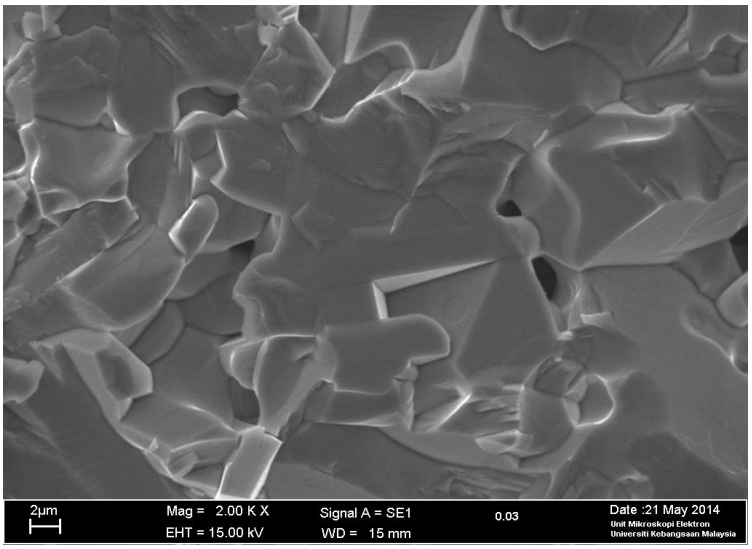

(b) x = 0.03

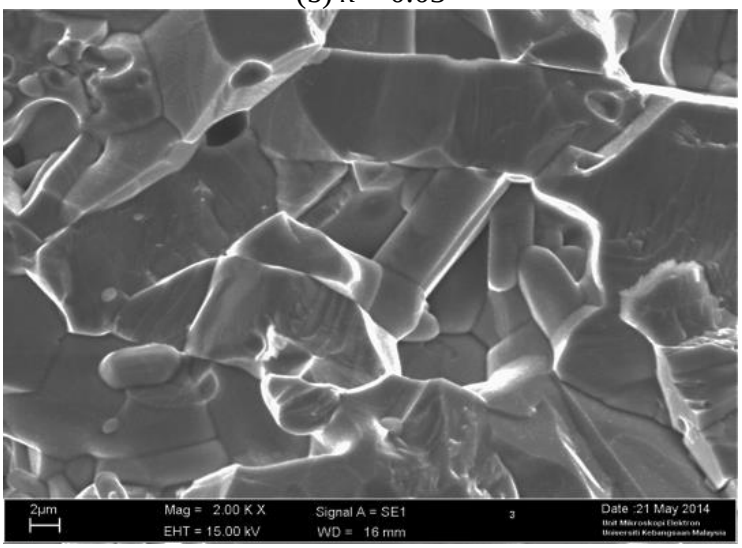

(c) x = 0.20

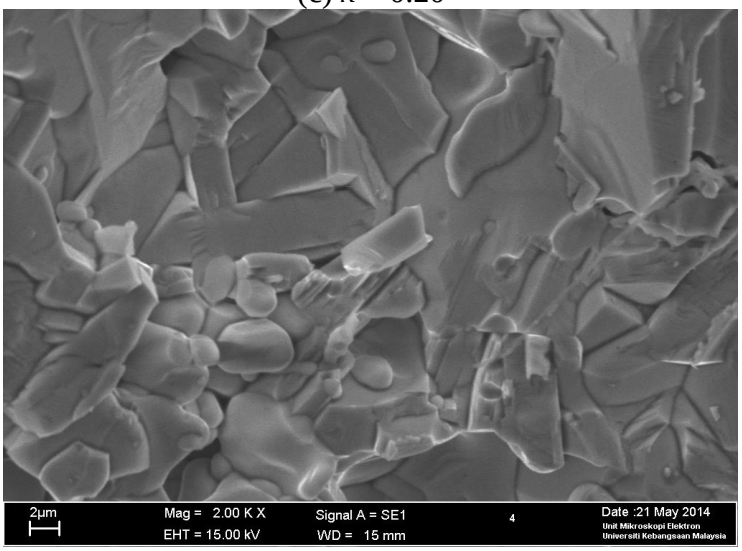

(d) x = 0.25

Figure 3. SEM micrographs of nano-sized PbO added $YBa_2CuO_{7-\delta}$ for x = (a) 0 wt. %, (b) 0.03 wt. %, (c) 0.20 wt. % and (d) 0.25 wt. %.

The lattice constants *c* increased while the *a* and *b* lattice constant showed very little change with PbO addition. The orthorhombic structure was maintained throughout the PbO addition range. Figure 3 shows that there is slight reduction in the grain size as PbO was added into the YBCO samples. The grain boundaries were also modified as a result of a slight partial melting.

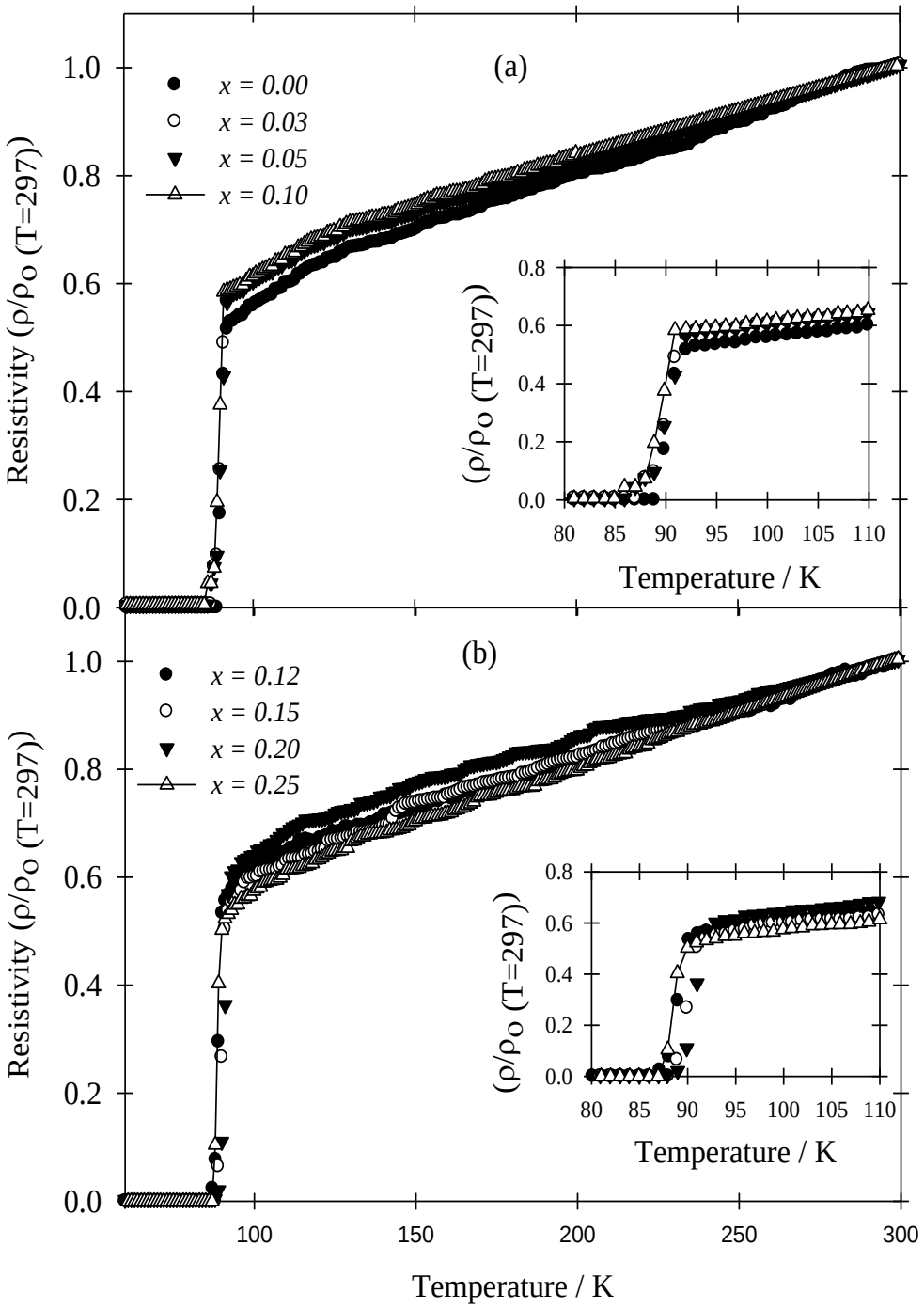

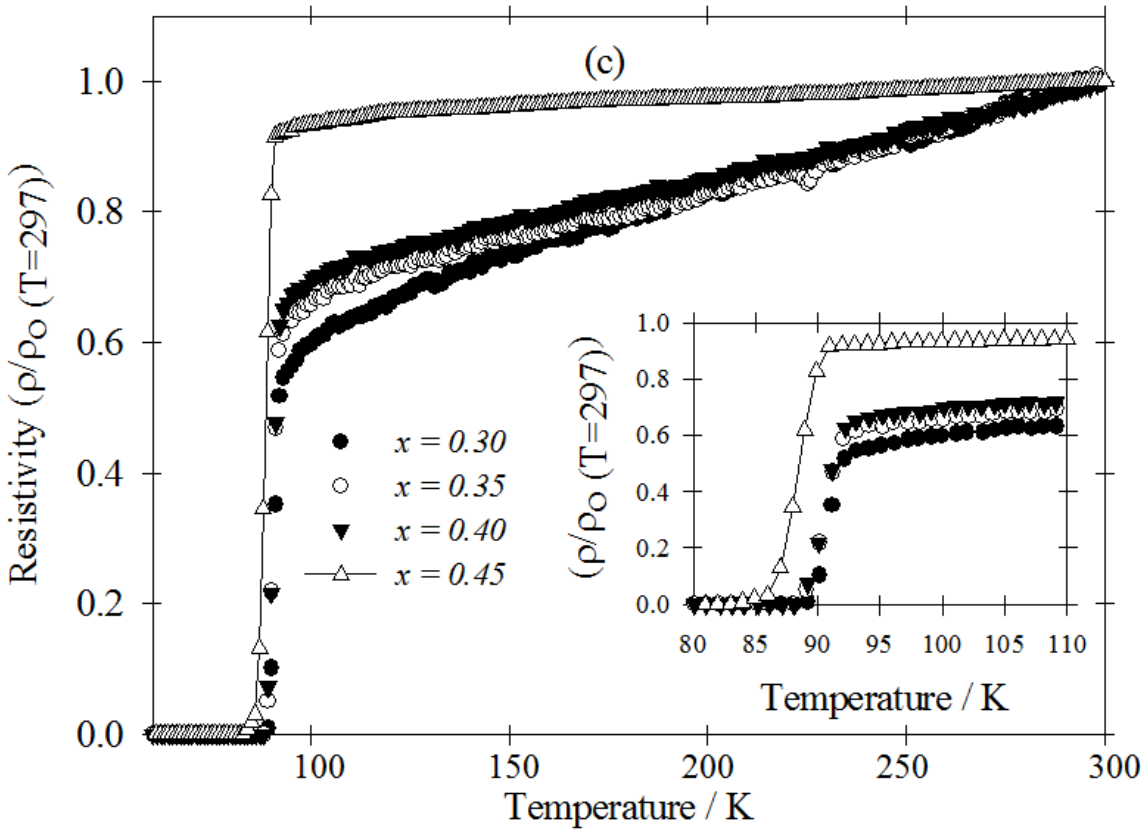

Figure 4. Resistivity ($\rho/\rho_{(T=297)}$) versus temperature curves of nano-sized PbO added $YBa_2CuO_{7-\delta}$ for x = (a) 0 to 0.10 wt. %, (b) 0.12 to 0.25 wt. % and (c) 0.30 to 0.45 wt. %

The resistivity-temperature curves of the samples are shown in Figure 4. All samples showed metallic normal-state behavior (i.e. $d\rho/dt > 0$) and a superconducting transition to zero resistance. Sample with x = 0.35 wt. % showed the highest $T_{c\ onset}$ = 94 K. PbO-addition does not substantially influence $T_{c\ onset}$; there is little variation ($T_{c\ onset}$ =91-94K) for all samples. The zero-resistance temperature ($T_{c\ zero}$), was lowest for x = 0.45 wt. % which showed $T_{c\ zero}$ = 84 K. Room-temperature resistivity increased with PbO content for x = 0.00 – 0.45 wt. %. Sample with x = 0.45 wt. % showed the highest room temperature resistivity (10.9 mΩ cm). The resistivity values indicate variation in the carrier concentration of $YBa_2Cu_3O_{7-\delta}(PbO)_x$. The $T_{c\ onset}$, $T_{c\ zero}$ and the room-temperature resistivity are shown in Figure 5.

Results of excess conductivity from the analysis of the superconducting transition curve has been described elsewhere [18]. In this paper we present results on the transport critical current density and flux pinning analysis.

Figure 6 shows J_c versus PbO content at 30 and 77 K. Figure 7 shows that the J_c decreases linearly with temperature for most of the samples, which indicates the flux pinning, created by a linear correlated disorder. The x = 0.25 wt.% sample showed the highest J_c (0.354 and 0.331 A/cm^2 at 30 and 77 K, respectively). For x = 0.45 wt.%, J_c decreased to 0.092 A/cm^2 at 77 K. J_c of the non-added sample is 0.079 and 0.058 A/cm^2 at 30 and 77 K, respectively. The J_c of the non-added samples was

of the same magnitude with previously reported values in polycrystalline copper oxide-based high temperature superconductors [19, 20].

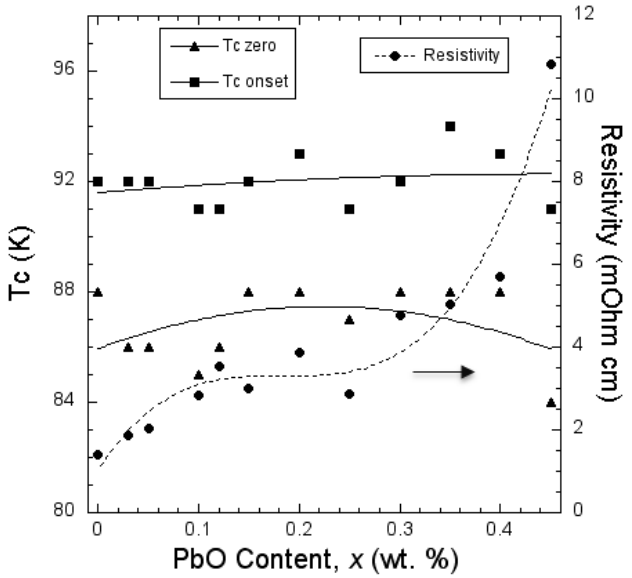

Figure 5. Normal state electrical resistivity (●) at 297 K and the variation of $T_{c\ onset}$ (■) and $T_{c\ zero}$ (▲) as a function of nano-sized PbO addition in $YBa_2CuO_{7-\delta}$

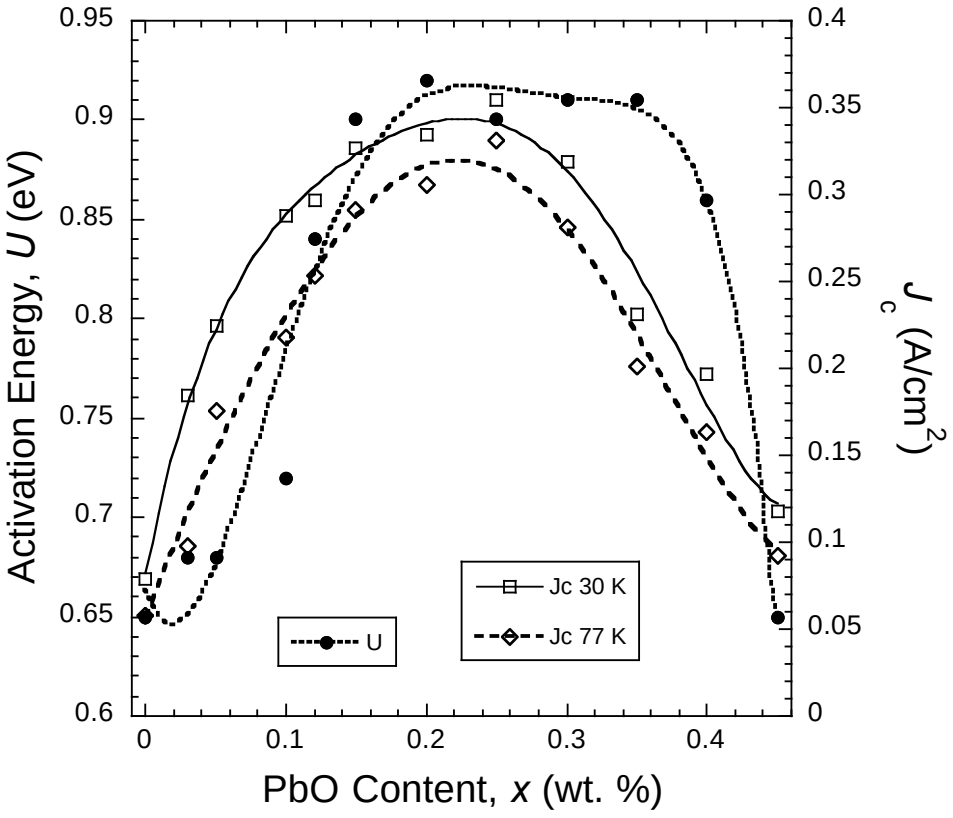

Figure 6. Critical current density J_c at 30 and 77 K and flux activation energy U as a function nano-sized PbO addition in $YBa_2CuO_{7-\delta}$

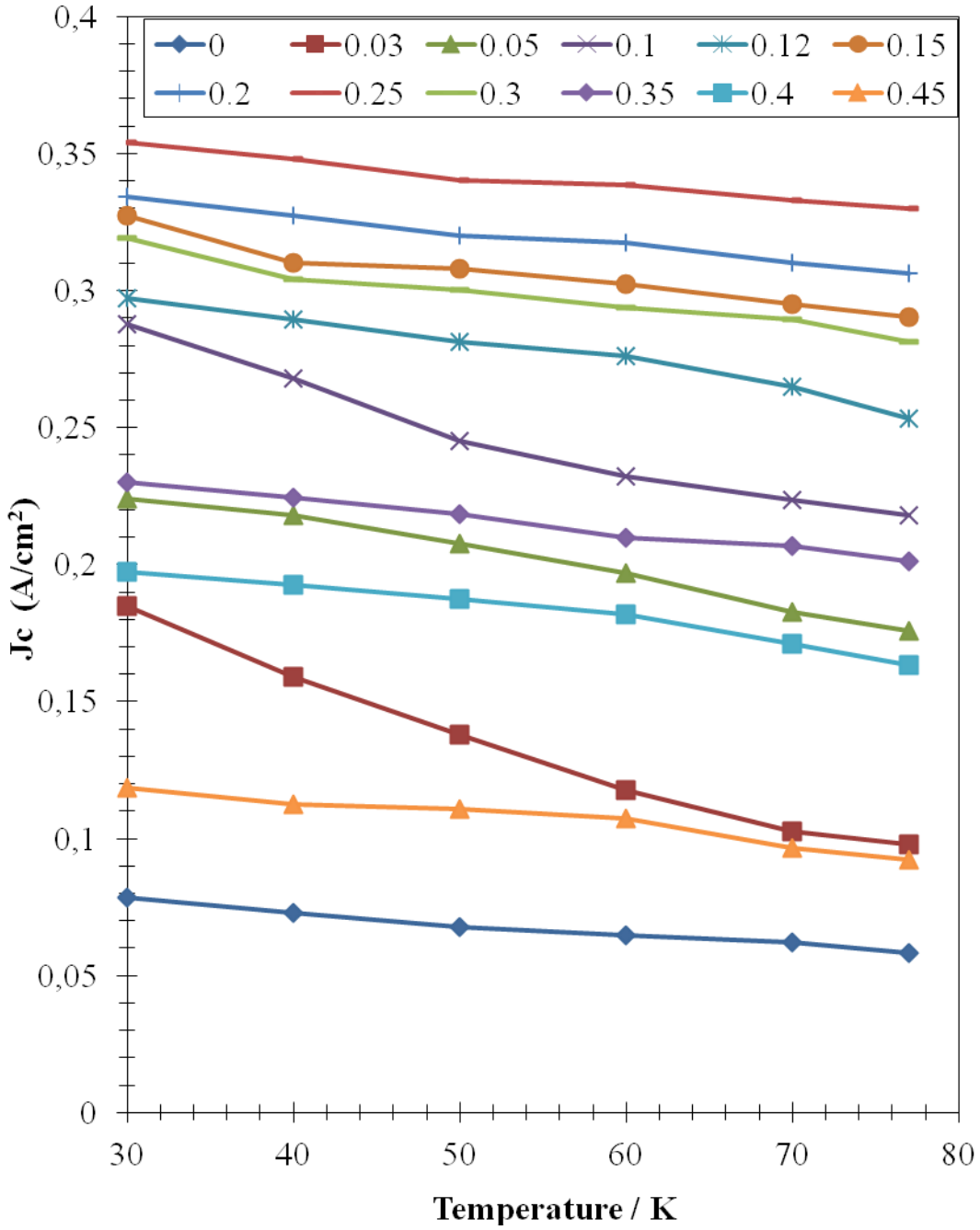

Figure 7. Critical current density J_c as a function of temperature for $YBa_2CuO_{7-\delta}$ (x = 0 – 0.45)

The pinning potential that can prevent vortex flow is due to a factors such as point-like defects and defects in the microstructure. The $ln(\rho/\rho_o)$ vs. $1/T$ plots for non-added and nano-sized PbO addition showed a non-linear behavior (Figure 8). According to the thermally activated flux creep model, the dissipated energy in the tail part of the resistivity plot is defined by an Arrhenius-type equation [7, 21-23]:

$$\rho(H, T) = \rho_o \exp [-U(H) / k_B T] \quad (1)$$

where U is the activation energy for flux creep, T is the temperature, H is the applied magnetic field, ρ_o is the pre-exponential constant and k_B is Boltzmann constant. In this work, the measurements

were made in zero fields (H = 0 T). The activation energy can be determined directly from the slope of the plot of $\log(\rho/\rho_o)$ versus $1/T$ as shown in Figure 8. In this work we have used the resistivity at 91 K as the value of ρ_o.

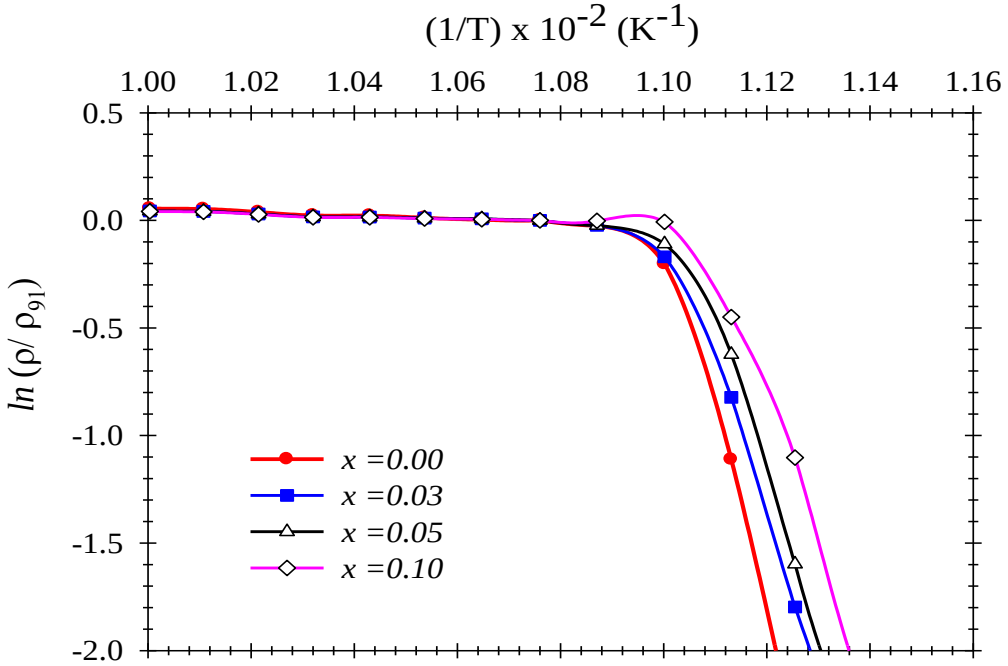

(a)

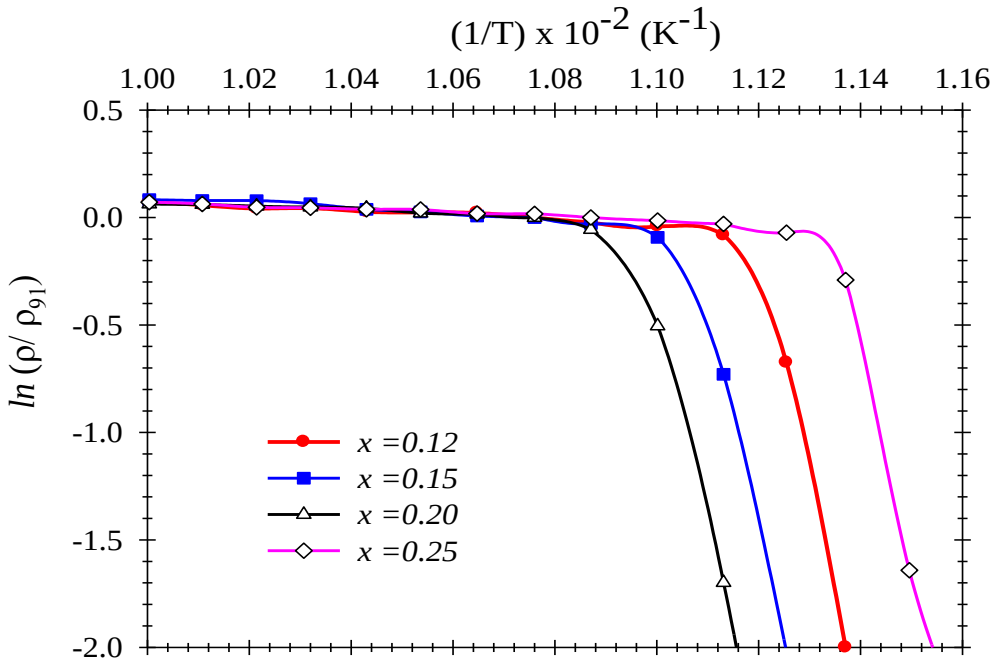

(b)

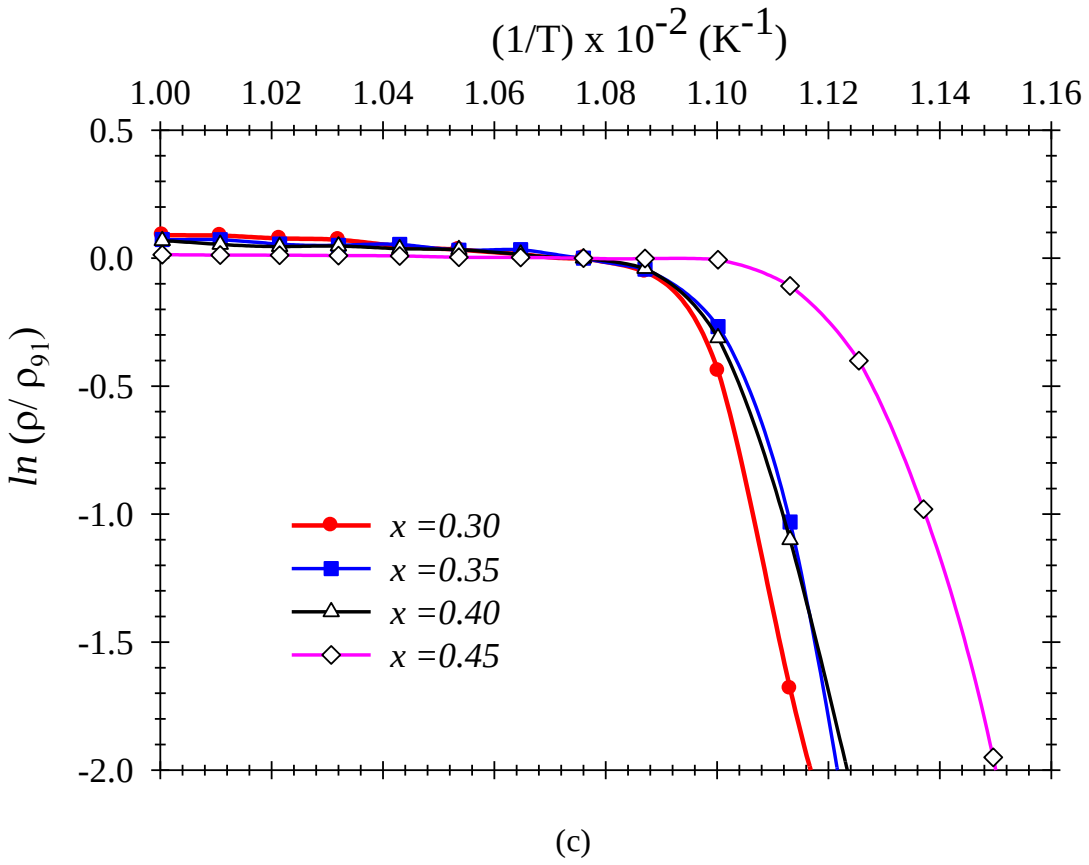

(c)

Figure 8. Arrhenius plot of the resistivity of $(YBa_2Cu_3O_{7-\delta})(PbO)_x$ (a) x = 0 to 0.10 , (b) x = 0.12 to 0.25 and (c) x = 0.3 to 0.45

Figure 6 shows the calculated activation energy from the linear data in the tail part of the plots (see Figure 8). The activation energy of the samples increased significantly with PbO nano-particle addition level up to x = 0.35 wt. % (U = 0.90 eV). The activation energy calculated for these samples is of the same order of magnitude reported in the potassium and cerium doped $Bi_2Sr_2CaCu_2O_{8+y}$ superconductor in zero fields (0.30 – 1.46 eV) [15, 24]. Changes in the grain boundaries and a reduction of the intergranular coupling and an increase in the amount of weak links can increase the activation energy [8].

In conclusion, sample with x = 0.35 wt. % showed the highest $T_{c\ onset}$ (94 K). J_c was highest at x = 0.25 wt. % which coincided with the highest activation energy (U = 0.90 eV) that showed a plateau between x = 0.20 and 0.35 wt. %. Maximum J_c at x = 0.25 wt. % can be explained as the increase in the flux activation energy as a result of nano PbO addition. Addition of nano-sized PbO up to x = 0.35 wt. % enhanced U which indicated an increase in the slope of the energy barriers. Sample with x = 0.25 wt.%, showed the highest J_c (0.354 and 0.331 A/cm^2 at 30 and 77 K, respectively) corresponding to activation energy U near the maximal value of 0.90 eV.

ACKNOWLEDGEMENTS

The authors thank the Ministry of Higher Education of Malaysia for supporting this work under grant no. FRGS/2/2013/SG02/UKM/01/1 and Universiti Kebangsaan Malaysia under grant no. DPP-2015-036 and GP-K005338.

References

1. Y. Zhao, C.H. Cheng and J.S. Wang, *Supercond. Sci. Technol.* 18 (2005) S43.
2. T.A. Campbell, T.J. Haugan, I. Maartense, J. Murphy, L. Brunke and P.N. Barnes, *Phys. C (Amsterdam, Neth.)* 423 (2005) 1.
3. Z.H. He, T. Habisreuther, G. Bruchlos, D. Litzkendorf and W. Gawalek, *Phys. C (Amsterdam, Neth.)* 325 (2001) 277.
4. Nasri A-Hamid and R. Abd-Shukor, *J. Mater. Sci.* 35 (9) (2000) 2325.
5. R. Abd-Shukor, I. Kong, E.L. Lim, N.A. Mizan, H. A., Alwi, M. H. Jumali, W. Kong, *J. Supercond. Novel Magn.* 25 (2012) 957.
6. N. Moutalibi and A. M Chirgui, *J. Phys.: Conf. Ser.* 97 (2008) 012284-1.
7. P.W. Anderson, *Phys. Rev. Lett.* 9 (1962) 309.
8. M. Erdem, O. Özturk, E. Yucel, S. P. Altintas, A. Varilci, C. Terzioğlu and I. Belenli, *Phys. B (Amsterdam, Neth.)* 406 (2001) 705.
9. D. H. Kim, K. E. Gray, R. T. Kampwirth and D. M. McKay, *Phys. Rev. B* 42 (1990) 6249.
10. D. Sharma, R. Kumar and V.P.S. Awana, *Solid State Commun.* 152 (2012) 941.
11. T.T.M. Palstra, B. Batlogg, R.B. Van Dover, L.F. Schneemeyer and J.V. Waszczak, *Appl. Phys. Lett.* 54 (1989) 763.
12. M. Tinkham, *Phys. Rev. Lett.* 61 (1988) 1658.
13. M.R. Mohammadizadeh and M. Akhavan, *Phys. C (Amsterdam, Neth.)* 390 (2003) 134.
14. R.C. Ma, W.H. Song, X.B. Zhu, L. Zhang, S.M. Liu, J. Fang, J.J. Du, Y.P. Sun, C.S. Li, Z.M. Yu, Y. Feng and P.X. Zhang, *Phys. C (Amsterdam, Neth.)* 405 (2004) 34.
15. B.Özkurt and B.Özçelik, *J. Low Temp. Phys.* 156 (2009) 22.
16. R. Abd-Shukor and K.S. Tee, *J. Mater. Sci. Lett.* 17 (1998) 103.
17. Ramin Yousefi, Farid Jamali Sheini, Abdolhossein Sa´Aedi and Mohsen Cheraghizade, *Sains Malays.* 44 (2015) 291.
18. Annas Al-Sharabi, Sarah Yasmin Tajuddin, Au Diya Fatihah Wan Saffiey, Syazana Jasman, H.A. Alwi, M.H. Jumali & R. Abd-Shukor. Excess Conductivity Analysis of PbO Nanoparticle Added $YBa_2Cu_3O_{7-\delta}$ Superconductor (in Malay), *Sains Malays.* (2016) doi:10.17576/jsm-2016-4512-21.
19. K.E. Oldenburg and W. A. Morrison, *Am. J. Phys.* 61(9) (1993) 832.
20. M. Anis-ur-Rehman and M. Mubeen, *Synth. Met.* 162 (2012) 1769.
21. P. W. Anderson and Y. B. Kim, *Rev. Mod. Phys.* 36 (1964) 39.
22. Bekir Özçelik, Hakan Gündoğmuş, Duygu Yazıcı, *J. Mater. Sci.: Mater. Electron.* 25 (2014) 2456.
23. B. Özçelik, E. Yalaz, M. E. Yakıncı, A. Sotelo, M. A. Madre, *J. Supercond. Novel Magn.* 28 (2015) 553.
24. B. Özçelik, C. Kaya, H. Gündoğmuş, A. Sotelo and M.A. Madre, *J. Low Temp. Phys.* 174(3-4) (2014) 136.